Table 1. DEM simulation parameters for FCC, RMD and RML samples.

| Samples | Parameter | Value |
|---|---|---|
| FCC | Particle size, $d_p$<br>Number of particles | 2.54 $(mm)$<br>3200 |
| RMD and RML | Particle size, $d_p$<br>Number of particles | 2.3-2.7 $(mm)$<br>34986 |
| FCC, RMD and RML | Particle density, $\rho_p$<br>Particle shear modulus, $G_p$<br>Particle Poisson's ratio, $v_p$<br>Transmitter frequency, $f$<br>Transmitter amplitude, $A$ | 2230 $(kg/\mathrm{m}^3)$<br>$25 \times 10^9$ $(Pa)$<br>0.2<br>20 $(kHz)$<br>2.5 $(nm)$ |

Table 2. Summary of exponents depending on correction adopted.

| $F(e)$ | $n_{prop}$ | $n_{osc}$ | $n_{third}$ |
|---|---|---|---|
| $B = 1.186$ | 0.12 | 0.18 | 0.05 |
| $B^* = 1.484$ | 0.17 | 0.15 | 0.03 |
| $B$ $varied$ $with$ $p'$ | 0.07 | 0.12 | -0.01 |
| $B = 1.186$, $C_N$ | 0.13 | 0.17 | 0.05 |
| $B^* = 1.484$, $C_N^*$ | 0.16 | 0.15 | 0.03 |
| $B$ $varied$ $with$ $p'$, $C_N$ | 0.07 | 0.12 | -0.01 |

Table 3. Summary of errors $\frac{\left|G_{oscprop}^{DEM} - G_{oscprop}^{regression}\right|}{G_{oscprop}^{regression}}$ using various void ratio corrections

| $\mathrm{F(e)} = \frac{(B-e)^2}{1+e} C_N^{\alpha}$ | $\frac{mean\left\|G_{oscprop}^{DEM} - G_{oscprop}^{regression}\right\|}{G_{oscprop}^{regression}}$ | $\frac{max\left\|G_{oscprop}^{DEM} - G_{oscprop}^{regression}\right\|}{G_{oscprop}^{regression}}$ |
|---|---|---|
| $B = 1.186$ | 0.0193 | 0.0637 |
| $B^* = 1.484$ | 0.0209 | 0.0573 |
| $B$ $varied$ $with$ $p'$ | 0.0130 | 0.0889 |
| $B = 1.186$, $C_N$ | 0.0177 | 0.0797 |
| $B^* = 1.484$, $C_N^*$ | 0.0142 | 0.0595 |
| $B$ $varied$ $with$ $p'$, $C_N$ | 0.0106 | 0.0669 |

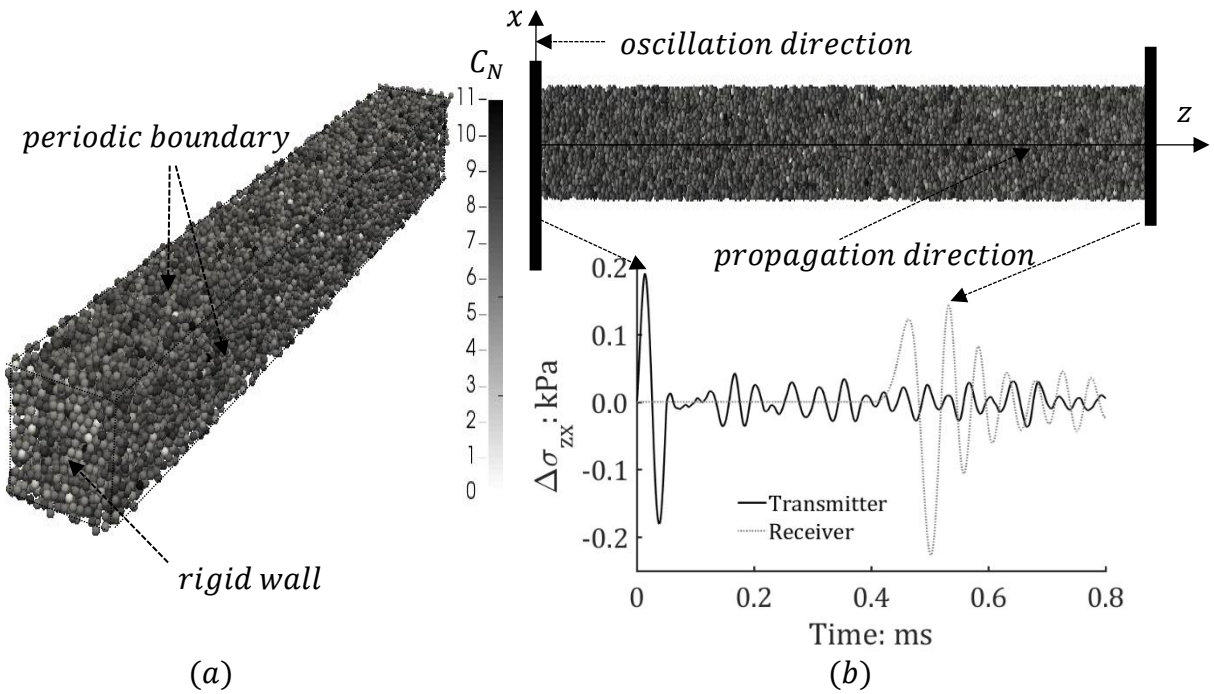


**Figure 1** Random packings with boundary conditions (a) $\boldsymbol{C_N}$ of dense sample at isotropic compression, $\boldsymbol{p'}$ = 300 kPa (b) illustration of generating shear wave to measure $\boldsymbol{G_{zx}}$ based on changes in shear stress on both rigid walls.

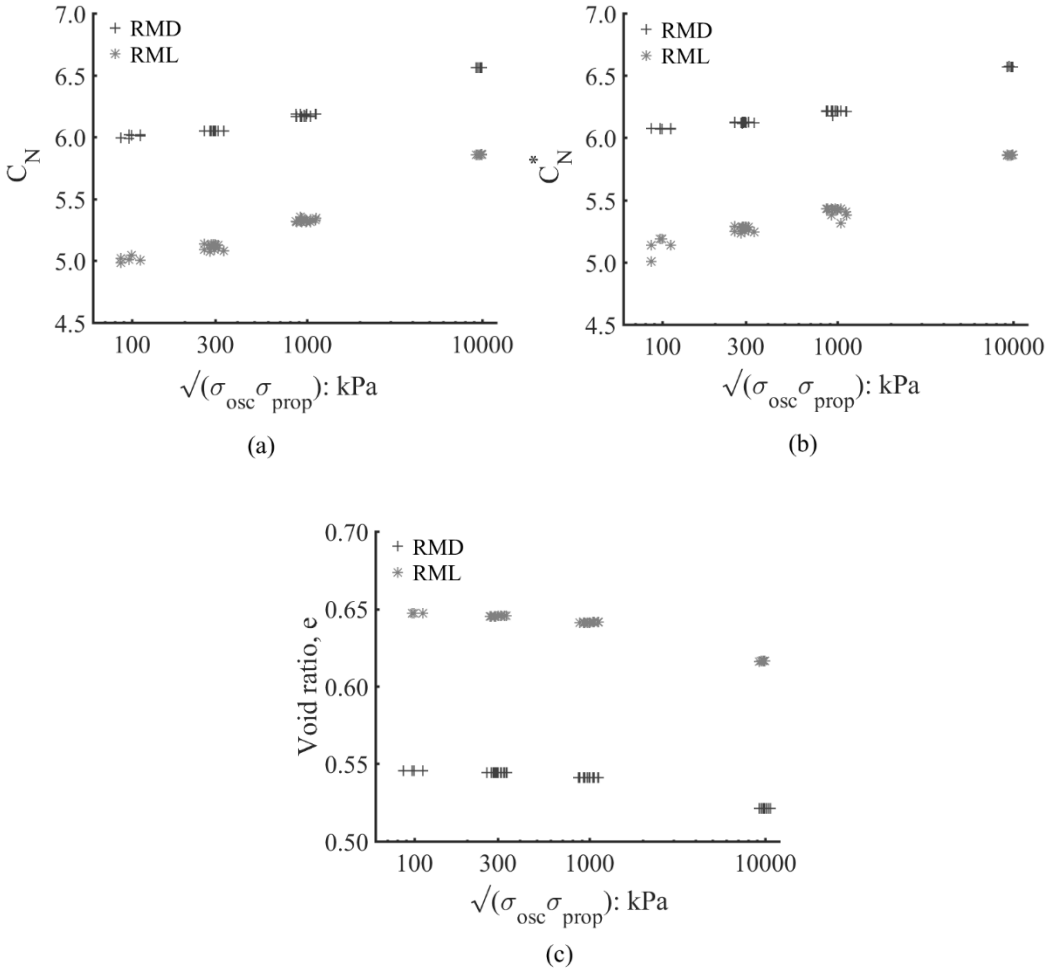


**Figure 2** Coordination number and void ratio at the start of shearing for samples considered (a) $\boldsymbol{C_N}$ versus geometric mean of geometric mean of the stresses in oscillation and propagation directions ($\sqrt{\boldsymbol{\sigma_{osc}\sigma_{prop}}}$ ) (b) $\boldsymbol{C^*_N}$ (mechanical coordination number) versus $\sqrt{\boldsymbol{\sigma_{osc}\sigma_{prop}}}$ (c) Void ratio versus $\sqrt{\boldsymbol{\sigma_{osc}\sigma_{prop}}}$

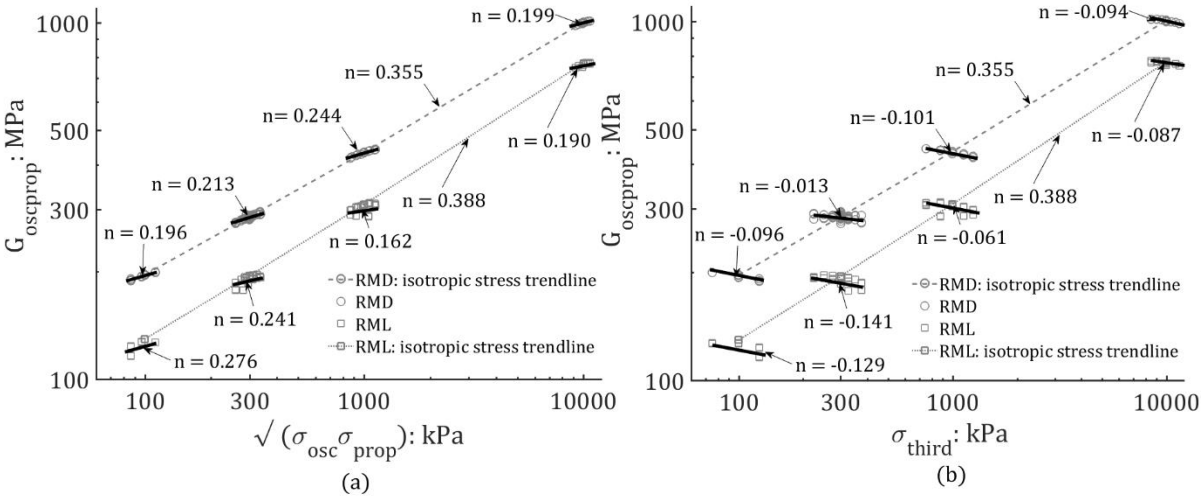


**Figure 3** Variation in $\boldsymbol{G_{oscprop}}$ with anisotropic stress state: (a) $\boldsymbol{G_{oscprop}}$versus geometric mean of stresses in oscillation and propagation directions ($\sqrt{\boldsymbol{\sigma_{osc}\sigma_{prop}}}$ ) (b) $\boldsymbol{G_{oscprop}}$ versus stress orthogonal to plane of propagation ($\boldsymbol{\sigma_{third}}$)

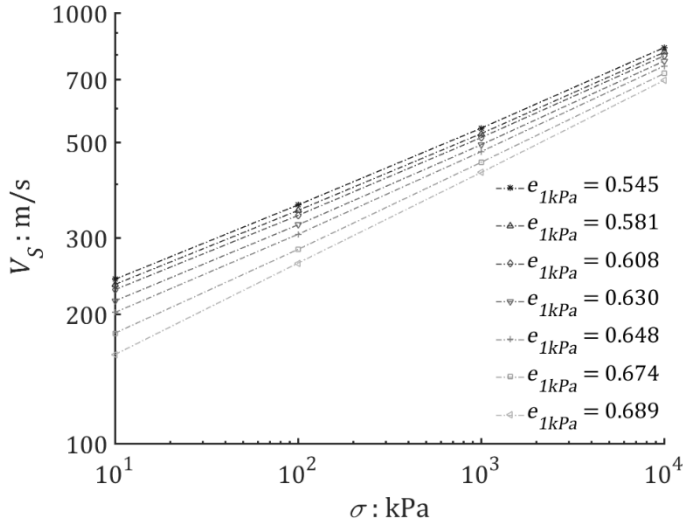


**Figure 4** Variation in shear wave velocities with isotropic stress

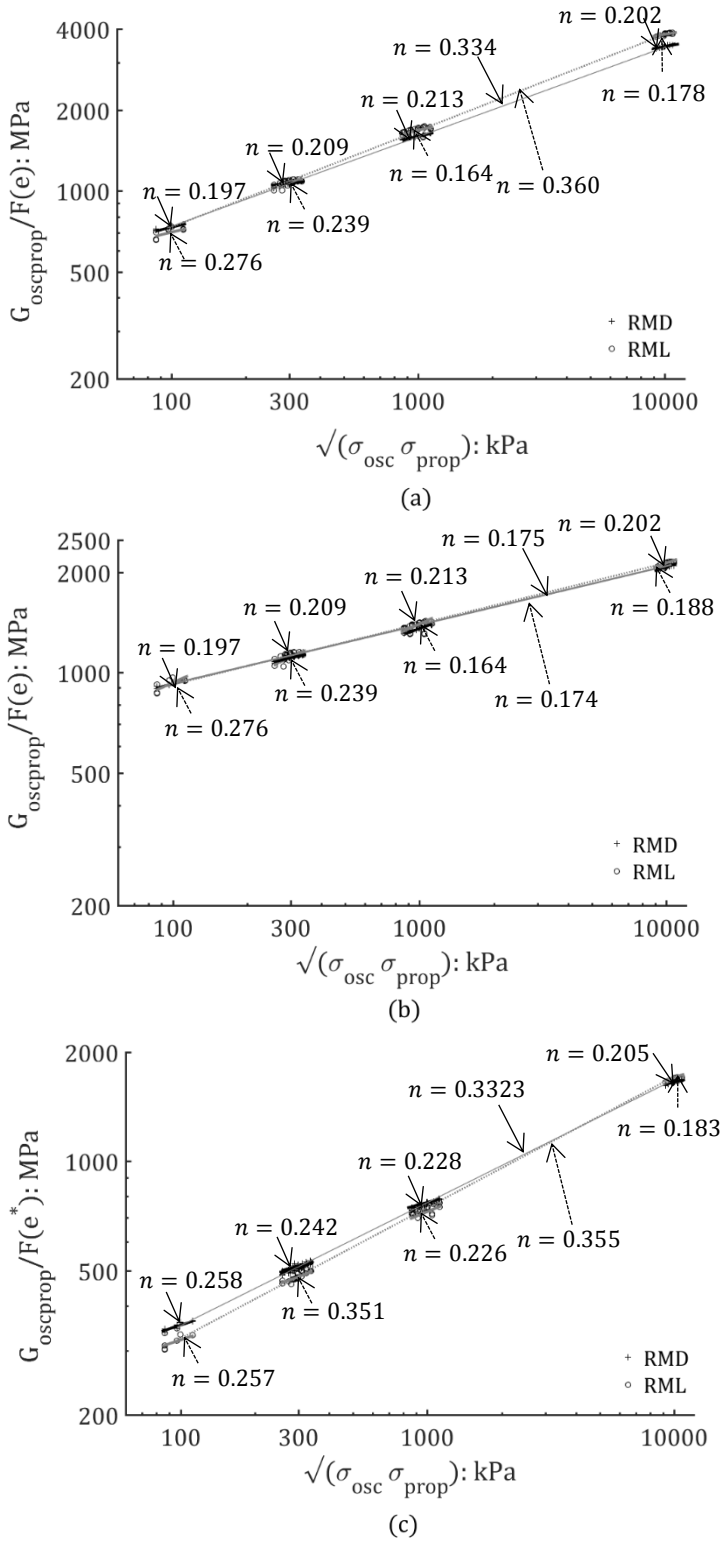


**Figure 5** Sensitivity of the relationship between the normalized shear modulus and $\sqrt{\boldsymbol{\sigma_{osc}\sigma_{prop}}}$ to the void ratio correction function chosen: (a) $\boldsymbol{G_{oscprop}/\mathrm{F}(\mathbf{e}, \mathbf{B} = 1.186)}$ versus $\sqrt{\boldsymbol{\sigma_{osc}\sigma_{prop}}}$ (b) $\boldsymbol{G_{oscprop}/\mathrm{F}(e, \mathbf{B\ varied})}$ versus $\sqrt{\boldsymbol{\sigma_{osc}\sigma_{prop}}}$ (c) $\boldsymbol{G_{oscprop}/\mathrm{F}(\mathbf{e}^*, \mathbf{B}^* = 1484)}$ versus $\sqrt{\boldsymbol{\sigma_{osc}\sigma_{prop}}}$

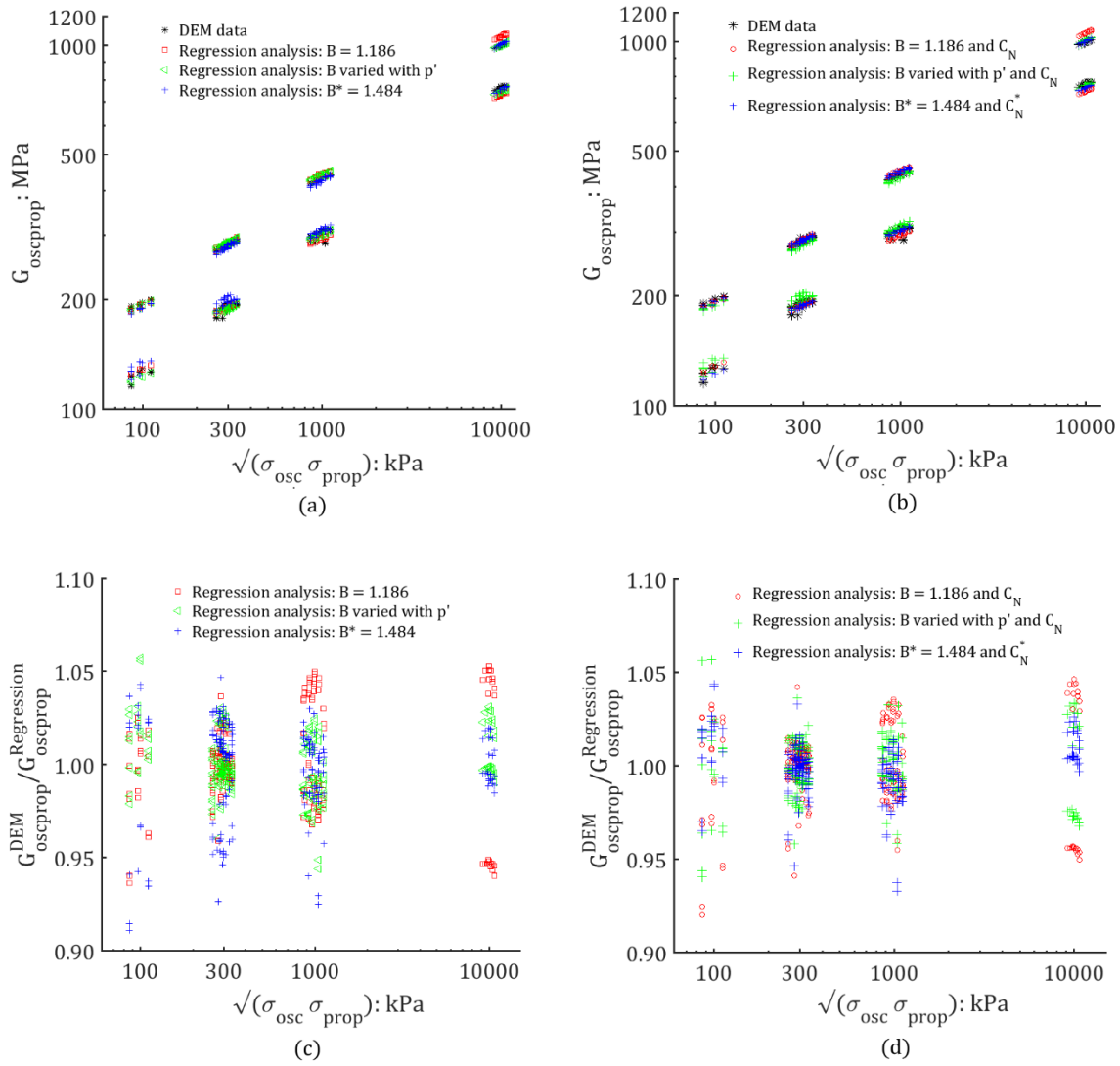


**Figure 6** Exploration of packing density correction functions by comparison of regression analysis data with data from DEM simulations: (a) $G_{oscprop}$ versus $\sqrt{\sigma_{osc}\sigma_{prop}}$ (b) $G_{oscprop}$ versus $\sqrt{\sigma_{osc}\sigma_{prop}}$ including $C_N^*$ *and* $C_N$ (c) $G_{oscpprop}^{DEM}/G_{oscpprop}^{Regression}$ versus $\sqrt{\sigma_{osc}\sigma_{prop}}$ (d) $G_{oscpprop}^{DEM}/G_{oscpprop}^{Regression}$ versus $\sqrt{\sigma_{osc}\sigma_{prop}}$ including $C_N$

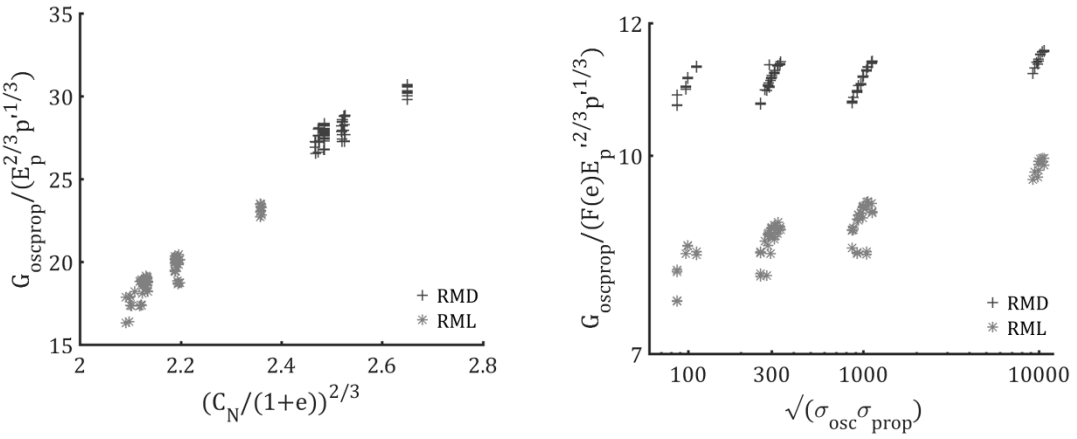


(a) (b)

**Figure 7** (a) Sensitivity of the relationship between the normalized shear modulus by $F(e) = C_N/(1+e))^{2/3}$and $\sqrt{\sigma_{osc}\sigma_{prop}}$ (b) Plot of $G_{zx}$ normalized by particle stiffness and mean effective stress versus $C_N/(1+e))^{2/3}$

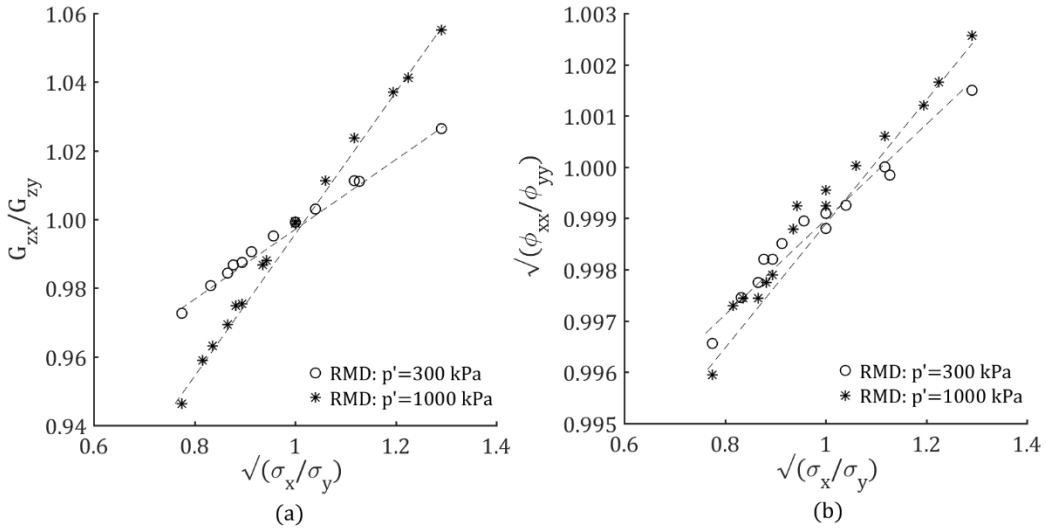


**Figure 8** Comparison of stiffness and fabric anisotropies with stress anisotropies (a) Variation in $\boldsymbol{G_{zx}/G_{zy}}$ with $\sqrt{\boldsymbol{\sigma_x/\sigma_y}}$ (b) Variation in $\sqrt{\boldsymbol{\phi_{xx}/\phi_{yy}}}$ with $\sqrt{\boldsymbol{\sigma_x/\sigma_y}}$